TRABAJO FIN DE MÁSTER

MÁSTER UNIVERSITARIO EN BIOTECNOLOGÍA Y BIOINGENIERÍA

CURSO 2019-20

UNIVERSIDAD MIGUEL HERNÁNDEZ DE ELCHE

NEURON AND GLIAL ACTIVATION ASSOCIATED WITH ACUTE MICROSTIMULATION IN THE PRIMARY VISUAL CORTEX

Autor: Charly Iglesias

Tutor académico: Prof. Dr. Eduardo Fernández Jover

Co-tutores: Prof. Cristina Soto Sanchez y Marcos Adrian Villamarin Ortiz

Declaration of the tutor

D. Eduardo Fernández Jover, Catedrático del Departamento de Histología y Anatomía de la Universidad Miguel Hernández y Director de la Unidad de Neuroingeniería y Neuroprótesis del Instituto de Bioingeniería de la Universidad Miguel Hernández de Elche.

CERTIFICA

Que el presente trabajo titulado:

"NEURON AND GLIAL ACTIVATION ASSOCIATED WITH ACUTE MICROSTIMULATION IN THE PRIMARY VISUAL CORTEX"

y que constituye la Memoria del Trabajo Fin de Máster en Biotecnología y Bioingeniería, que presenta:

Charly Iglesias

ha sido realizado bajo su supervisión en el Instituto de Bioingeniería, cumpliendo todos los requisitos necesarios.

Y para que así conste, se expide y firma el presente certificado en Elche a 26 de junio de 2020

Fdo.: Prof.Eduardo Fernández Jover

Abstract

- **Background.** Sensory handicaps such as blindness significantly decrease life quality, and the development of a navigational form of sight through cortical stimulation represents a massive breakthrough towards improving these people's lives. The use of cortical prosthesis capable of stimulating electrically the visual area of the brain could potentially evoke visual perceptions(1). However, immune response against the device limits data acquisition and an accurate stimulation of the brain, preventing the development of a fully functional cortical prosthesis.
- **Methods**. A stiff stimulating-capable electrode was implanted in V1 of rats and used to study brain-technology interaction, specifically **neural activation** and **glial activation** (Astrocytes and Microglia). To address this, three conditions were considered, **'electrode implantation with stimulation'**, **'electrode implantation without stimulation'** and **'no electrode implantation'**[1].
- **Results.** Both neuron and glial populations exhibited an increased activation associated with acute microstimulation and electrode insertion around the electrode's site.
- **Conclusions.** Our results indicate a correlation between acute **microstimulation** in the primary visual cortex of rats and an increased **neuron and glial activation**.

[1] "No electrode implantation" condition was performed only for neural activation analysis.

Key words

-MEA: Multi-Electrode Array

-UEA: Utah Electrode Array

-PBS: Phosphate buffered saline

-STT: Somatostatin

-GAD: GABA

-PV: Parvalbumin

Table of contents

Introduction and background

Sensory handicaps such as blindness are estimated to affect over **2,550,000** people in Europe and over **30 million** globally. According to the *World Health Organization*, visual impairment affects over **30 million** individuals in Europe, and due to the growing elderly population and other health factors, the tendency is increasing (2).

Blindness decreases life quality and increases unemployment and social exclusion. Consequently, it could trigger other disorders, such as depression. Uncovering how to cure blindness would not only improve these people's lives but also have positive economic repercussions since they would regain work capability and independence, requiring much less social care.

From a medical-engineering perspective, there are two main approaches for vision restoration, **Retinal Implants** and **Intracortical Visual Prostheses**. The most studied are Retinal Implants (primary stage of visual processing), which stimulate fine retinal neurons to elicit visual percepts. However, this approach would not successfully restore sight in patients without functional retinal neurons or injured at any other stage of the visual pathway.

By contrast, Intracortical Visual Prostheses attempt to successfully bypass the early vision pathway[2], providing treatment to arguably all blind patients by directly stimulating the brain's **early cortical visual processing areas** (V_1 and V_2) (4). Intracortical visual prostheses are generally conformed by a **camera,** which the user wears on a pair of glasses, a **processor** that transforms the camera footage (into an adequate cortex stimulation pattern), and the **intracortical implant** that delivers micro-electrical stimulation to the visual cortex.

The purpose of this is to evoke *phosphene* perception, a phenomenon in which light dots are perceived without depending on light getting through the eyes (5). This suggests the feasible generation of complex perceptions with multiple *phosphenes* for future navigational support applications and, in the longer term, to reliably restore sight (6).

[2] Including retina, optic nerve, chiasm, tract, lateral geniculate nucleus and optic radiations until visual cortex (3).

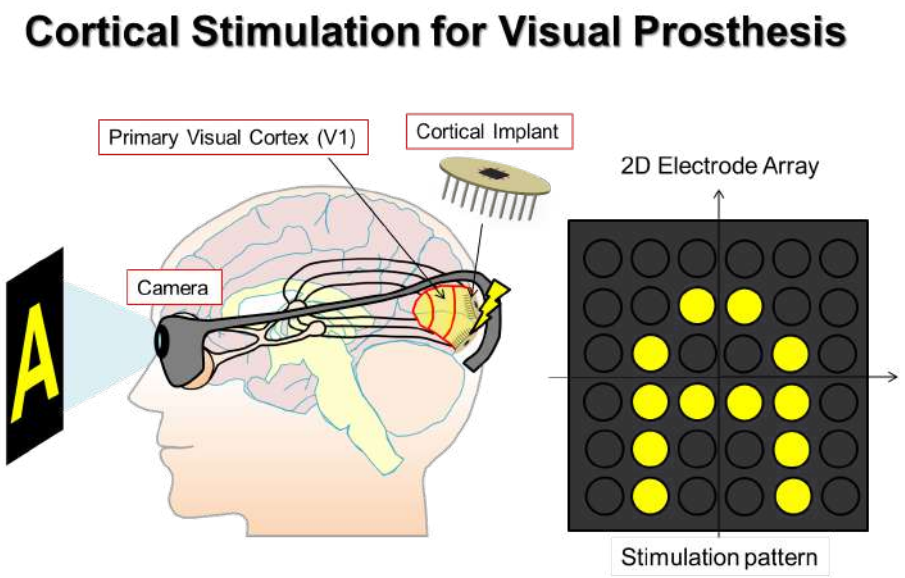

Fig.1 Cortical stimulation for visual prosthesis (7).

Besides micro-stimulation, intracortical prostheses are often capable of recording electrical signals within the brain down to the level of individual neurons.
They are generally used to record electrical signals from specific areas of the brain, which affords insight into the activity of specific populations of neurons, providing a valuable research tool in the field of sensorimotor and cognitive neuroscience (8,9).

Neural electrodes allow direct communication between device and brain, enabling being utilised in applications such as brain-machine interfaces (BMI), to record neural activity as an input signal, to decode and extract motor intended processes, behaviour/cognitive states and other desired actions for external devices (10). To study neural modulation algorithms and statistical methodologies are being developed to uncover meaningful spatiotemporal patterns of neural activity. Also, the inability to record from large numbers of neurons has limited the development of invasive BMIs, so huge efforts are currently being made to improve recording reliability and biocompatibility.
Clinically, the use of neural electrodes has been successfully implemented for the treatment of a number of neurological disorders, such as *Epilepsy*, *Parkinson's disease* and *Obsessive compulsive disorder* (11–13).
The gold standard for cortical single-unit recording and stimulation is the *Utah Electrode Array* (UEA), but since its development in 1997 (24 years ago), many other solutions have arisen, such as "flexible, soft and/or stretchable" bioelectronics, "micro or nano scale" probes and "biocompatible coating or drug release capability" among other features, seeking to minimise immune response (14).

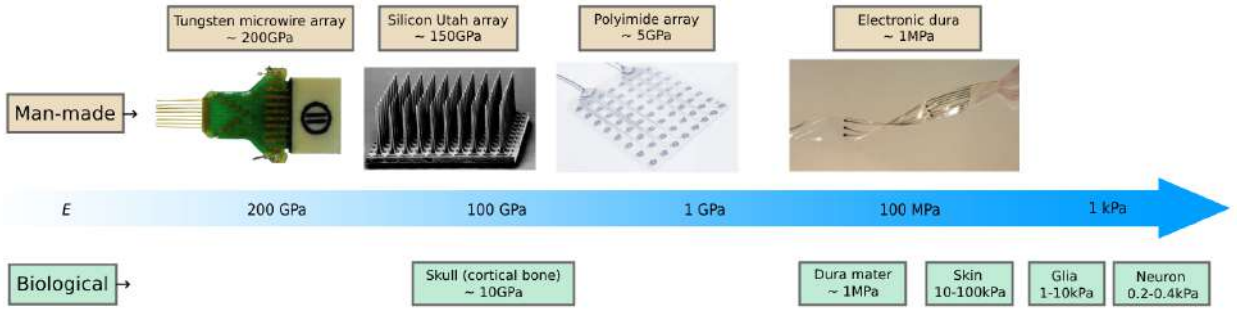

Fig. 2 Comparison between *Young's modulus* of invasive electrodes vs neural-related tissue.

Moreover, due to the geometrical inaccessibility of the brain, recordings from microelectrode arrays (MEA) have been combined with optogenetics enabling higher spatial resolution to differentiate cell types, shapes and connections. But flexible MEAs face many limitations, such as buckling during brain insertion and the unviable insertion of long-length flexible probes due to lack of accuracy in targeting specific regions in the brain (15). However, many efforts are being made for the development of novel flexible intracortical MEAs, since they elicit lower immune response and less tissue damage due to brain's micromotion (e.g. head movements and cardiac rhythms) presenting great potential for both brain research and the development of clinical neuroprosthetic devices (16).

They are a promising technology for both basic research and the development of clinical neuroprosthetic devices.

In the upcoming years, flexible MEAs could allow achieving a seamless brain-tissue interaction providing therapeutic uses to modulate neural activity or even sensory function, such as vision using a direct cortical interface (17).

There are many factors that hinder achieving long-term consistent neural recordings such as a limited or harmful stimulation, delamination and breakdown of the device, an inadequate tethering of the electrode, increasing impedance for scaling down to single neuron size, size mismatch, mechanical mismatch and the one of our concern, immune response (18,19). The foreign body response is characterised mainly by a neuroinflammatory tissue response to the microelectrodes (20) which in the cortex is characterised by the abundance of immune cells such as **glial cells**. This immune response is amplified when the electrode insertion or tissue compression ends up breaking blood vessels generating a haemorrhage (e.g. in the brain's parenchyma) and producing a bleeding in the tissue we are aiming to study.

To address this problem and **reduce glial response** and **inflammation**, different approaches have been proposed to reduce acute and chronic inflammatory reactions.

1. **Insulation coating biocompatibility**.
   Noble metals, such as platinum, iridium, and gold are commonly used materials for neural electrodes due to their biostability, electrical conductivity and corrosion resistance.

2. **Anti-inflammatory molecules release adhered to polymer-based electrode coatings**.
   Long-term implant stability depends on neuroinflammatory response, and this reaction could be controlled by using polymeric electrode coatings or by inoculating the anti-inflammatory

molecules directly through microchannels incorporated in the probes. Nanoparticles conjugated with drugs such as corticosteroids or immunosuppressants to improve the symbiosis between the electrode and the tissue have shown positive results (21).

3. **Drug release to suppress tissue response .**
   Drug release is also significantly relevant in order to improve the electrode's integration and performance. One approach focuses on electrode coating for local release of dexamethasone to control astrocytic response (22), however, the interference with other coatings and the amount of active compound charged in the coating are some of the problems that need to be addressed in order to meet the needs.

4. **An adequate morphology of the microelectrode.**
   Design of the shafts and tips are an important aspect of the design of intracortical probes, such as flexible electrode arrays, electrode size's reduction or tip's sharpness (23).
   The insertion of an ideal, ultrasharp, smooth array would pierce blood vessels without distorting or tearing the walls. By contrast, the insertion of a non-sharp tip would tear the vessel walls and could promote excessive bleeding. In both cases, the inherent probe's residual tension may be able to prevent some of the microhemorrhages in the surrounding tissue.
   Also, in order to register a large brain area, nanostructured electrodes with high electrochemical properties would be used as a neural interface obtaining a more stable signal.

5. **Insertion speed.**
   Electrode insertion will cause compression of the tissue, which may nick cell membranes altering cellular homeostasis due to ion leakage. This leakage could also potentially lead to cell death. An optimal insertion speed would avoid unnecessary tissue stretching.

6. **An optimised surgical procedure.**
   An adequate surgical procedure (e.g. adjusting insertion pressure) reduces some of the main negative effects of electrode implantation, like neural damage or haemorrhage produced by oedema or blood vessel rupture.

Furthermore, apart from neuroinflammatory response, there are far more issues to address while working on the development of intracortical visual prostheses such as **excitation propagation** in the cortical tissue. Cells near the microelectrode may get damaged due to inadequate pulse width and current density, producing a glial scar. Thus, it is important to develop stimulation protocols to minimise tissue damage and to allow them to work for prolonged periods of time.
Interestingly, in some cases, glial scarring benefits the implementation of neuroprosthesis, since after electrode implantation in the brain, microglial activation, reactive astrogliosis, and neuronal cell death create an environment surrounding the electrode, increasing its stability and tethering. However, this scar also hinders the transit of current needed for stimulation and recording purposes. Consequently, glial scar should always be avoided.

Depending on the role they perform, neurons from the cortex are divided in two groups, **excitatory** neurons and **inhibitory** neurons.

- **Excitatory neurons:** It is a kind of neuron that represents about the 80% of the neurons in the brain (in mammals), which is characterised by releasing neurotransmitters that fire action potentials in the postsynaptic neurons, causing the opening of sodium channels and thus transmitting a flow of information (24). The main excitatory neurotransmitter is *Glutamic acid,* although there are other neurotransmitters such as *epinephrine*, *norepinephrine* and *nitric oxide*.
  They can project within localised regions or long-range projections between different cortical areas.
  Excitatory neurons in the cortex are known as pyramidal neurons (25).
    - **Pyramidal neurons:** They are multipolar neurons[3] responsible for most excitatory functions in the brain.

- **Inhibitory neurons:** Representing about the 20% of the brain neurons, these are cells characterised by releasing neurotransmitters that inhibit action potentials, causing the opening of the channels and thus regulating the action of excitatory neurons (chloride channels among other mechanisms) (26). The most frequent inhibitory neurotransmitter is *gamma-aminobutyric acid* (GABA), although there are other kinds such as *dopamine, serotonin* and *glycine.*
  They only project within localised small areas and depending on the protein they express, there are three kinds of inhibitory neurons.
    - **Somatostatin (STT).**
    - **GABA (GAD)**
    - **Parvalbumin (PV)**

Furthermore, going back to the neuroinflammation, while trying to measure or quantify the immune response of the tissue, the most relevant are the following cell types:

- **Astrocytes:** Astrocytes are responsible for the maintenance of brain homeostasis. Both Astrocytes and neurons cooperate on several functions, such as neurotransmitter trafficking, ion homeostasis, defence against oxidative stress and control of the blood brain barrier and blood flow (27).

- **Microglia:** Microglia cells are a specialised population of macrophages-like cells in the central nervous system (CNS) being the main immune cells of the central nervous system. They consequently play important roles in brain infections and inflammation, they are immune sentinels capable of orchestrating a potent inflammatory response.
  During development and neurogenesis, microglia interactions with neurons help to shape the final patterns of neural circuits important for behaviour and with implications for diseases. Also according to the latest studies, microglia is involved in monitoring the integrity of synaptic function (28). In neuroinflammation, microglia shows longer ramification.

- **Neurons:** Neurons are electrically excitable cells that transmit signals throughout the body. They employ both chemical and electrical components in the transmission of information, and they are connected to other neurons at synapses and to effector organs or cells at neuroeffector junctions (29). During neuroinflammation, neurons exhibit an increased displacement around the electrode site.

[3] Neurons characterised by possessing a single axon and many dendrites

Neural activity means that the neurons send action potentials. An excessive neural activation could induce cell soma hypertrophy, neurovascular uncoupling[4] or even neuron's death (31,32).

To study neural activity due to acute stimuli expression, it is usual to identify the presence of c-Fos by immunohistochemical techniques. C–Fos is a protein that has been widely studied since it is expressed within some neurons following depolarization (33). It has been shown that different stimuli can induce c-Fos expression in the brain, and c-Fos immunostaining and in-situ hybridization are used to map brain metabolism (34).

Our research group decided to make different studies to determine the neuronal expression of c-Fos associated with the electrical stimulation of the brain using an intracortical electrode, considering as a control the insertion of the electrode without electrical stimulation. However, an unexpected finding was that only electrode insertion also exhibited c-Fos expression without stimulation, just by inserting the electrode. Due to this event, the experimental design was modified by adding a non-stimulation part to the analysis and using the contralateral[5] brain hemisphere as a control.

[4] It is a term that describes neuronal blood flow alterations associated with neuronal activity (30).

[5] Where the electrode wasn't implanted.

Objectives

The present study aims to study **neuron activation** and **glial activation** after acute brain microstimulation for further understanding of brain-electrode interaction, focused on the development of intracortical visual prostheses at the *Bioengineering Institute of the University Miguel Hernández*.

The main objectives of the present work are the following:

1. Studying **"neuron activation"**.
    a. Associated with the stimulation of an intracortical electrode (20/60 µA).
    b. Associated with the insertion of an intracortical electrode (0 µA).
    c. Control[6] | Without the insertion of an intracortical electrode.

2. Studying **"glial activation"**.
    a. Associated with the stimulation of an intracortical electrode (20/60 µA).
    b. Control | Associated with the insertion[7] of an intracortical electrode (0 µA).

Further details about the process are provided below:

Cortical response associated with the insertion of an electrode in the visual cortex.

A. **Cell activation with stimulation (20/60 µA).**
    i. **Inhibitory neurons.**
        1. Somatostatin (STT).
        2. GABA (GAD).
        3. Parvalbumin (PV).
    ii. **Glial cells**
        1. Astrocytes (GFAP)
        2. Microglia (Iba1)

B. **Control (Cell activation without stimulation[8]).**
    i. **Inhibitory neurons.**
        1. Somatostatin (STT).
        2. GABA (GAD).
        3. Parvalbumin (PV).
    ii. **Glial cells**
        1. Astrocytes (GFAP)
        2. Microglia (Iba1)

[6] Note: Unexpectedly, electrode insertion also exhibited c-Fos expression without stimulation. Due to this event, the experimental design was adapted by analysing the contralateral hemisphere as the new control, for further understanding.
[7] Contrary to neuron activation, glial activation was initially expected to happen as a consequence of electrode insertion.
[8] Electrode insertion without current delivery.

Experimental procedure

For the experimental procedure the type of approach implemented was in vivo testing, which implies the insertion of microelectrode probes in animal visual cortex, followed by the sacrifice and extraction of the histological samples, Immunohistochemistry, quantification and statistical analysis of the gathered data.

Animals and Surgical Approach

All animal experiments conducted in this study were carried out in conformity with directive 2010/63/EU of the European Parliament and of the European Council, and with Spanish regulation RD/53/2013 on the protection of animals in experiments for scientific purposes, and with the approval of the Ethics and Institutional Committee for the Use and Care of Animals of the Miguel Hernández University (UMH).

The animal model we used for this study consisted of 9 albino Wistar rats provided by the University's Animal Experimentation Unit. All animals weighed between 200-300g, they were randomly named, fed *ad libitum*, followed a day-night cycle of 12:12 (night-day) and they were kept under these conditions for 7 days prior to the surgery.
All rats were divided into three experimental groups:

- 20 µA (n=3)
- 60 µA (n=3)
- 0 µA (sham stimulation, n=3),

In all rats, electrode's insertion was performed in layer 4 of the primary visual cortex V1, located in the left hemisphere of the occipital lobe, anterior to the lambdoid commissure (AP -6.3 mm from bregma; ML 3 mm and 1.5 mm dorso-ventral) (35).

Implantation of intracortical electrodes[9]

The animals were initially sedated with Isoflurane 4% (IsoFlo® Zoetis, Parsippany, NJ.) and subsequently anaesthetised by inoculating intraperitoneally Xylazine (10mg/kg of Xilagesic) and Ketamine (70mg/kg of Ketamidor). Buprenorphine (0.03 mg/kg, subcutaneous) was administered to improve analgesic effect, and dexamethasone (1 mg/kg, intraperitoneal) to avoid oedema.

Isoflurane was administered after placing an anaesthetic mask to the rat through a gassing mask with a concentration of **2%**.
The electrode was introduced into a saline solution for operability verification and in a fluorescent solution for an easier probe's scar localisation during immunohistochemistry. The chosen intracortical electrode was a bipolar probe (stereotrode) configured by a shank manufactured in Platinum and Iridium, 0'216mm of diameter, a 50mm polyimide tubing and two blunt activated-iridium tips at 50kΩ of impedance with a separation of 75µm. (Science Products GmbH, ref PI2ST30.05B3, Germany).

[9]This surgical procedure has been performed in previous articles (36–38).

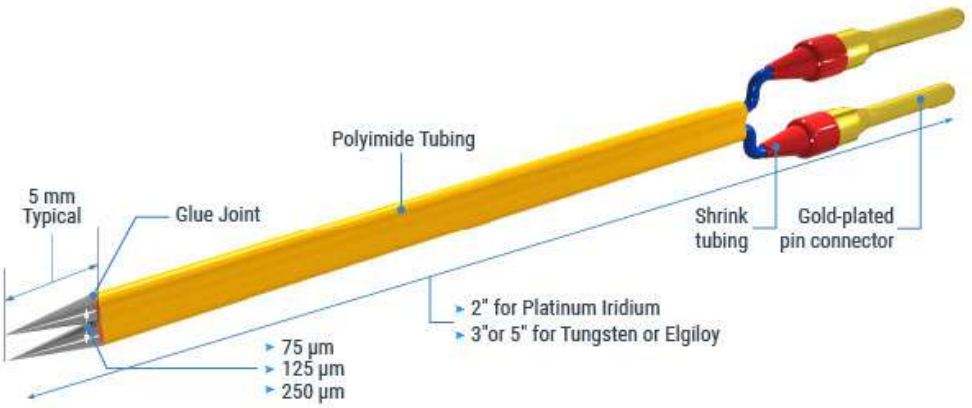

Fig. 3 Platinum-Iridium Bipolar Stereotrode's components (39).

This specific type of electrode was selected due to its impedance and morphological similarity with the electrodes found in the UEA.
In each procedure, the rat was placed on a heat-active surface to maintain its core temperature[10].
An optimal breath rate was maintained over the whole procedure and it was expected to decrease slightly over time (41). Besides the breath rate, the rat's *paw withdrawal reflex* was checked every 5 minutes by pressing the hind paws to determine anaesthesia depth throughout the procedure.
Moreover, since rodents often do not close their eyelids while being anaesthetised, physiological saline was applied every 5 minutes to the animal's eyes to prevent them from drying, which also allowed *palpebral reflex* checking for anaesthesia deepness monitorisation.

In order to localise the desired area and regulate the stereotactic frame, an Atlas (The Rat Brain in Stereotaxic Coordinates. London: Academic Press, 2007) of the rat brain was used, in which the rat brain was represented layered while providing functional information about all the areas. The skulls' anatomical reference point used for brain navigation was *Bregma*[11].

[10] Anaesthesia causes the redistribution of heat from core to periphery during surgery as a side effect (40).
[11] Bregma is an anatomical reference point often used for brain stereotactic surgery. It is located where the sagittal and coronal sutures intersect, on the calvaria's superior-middle portion (42).

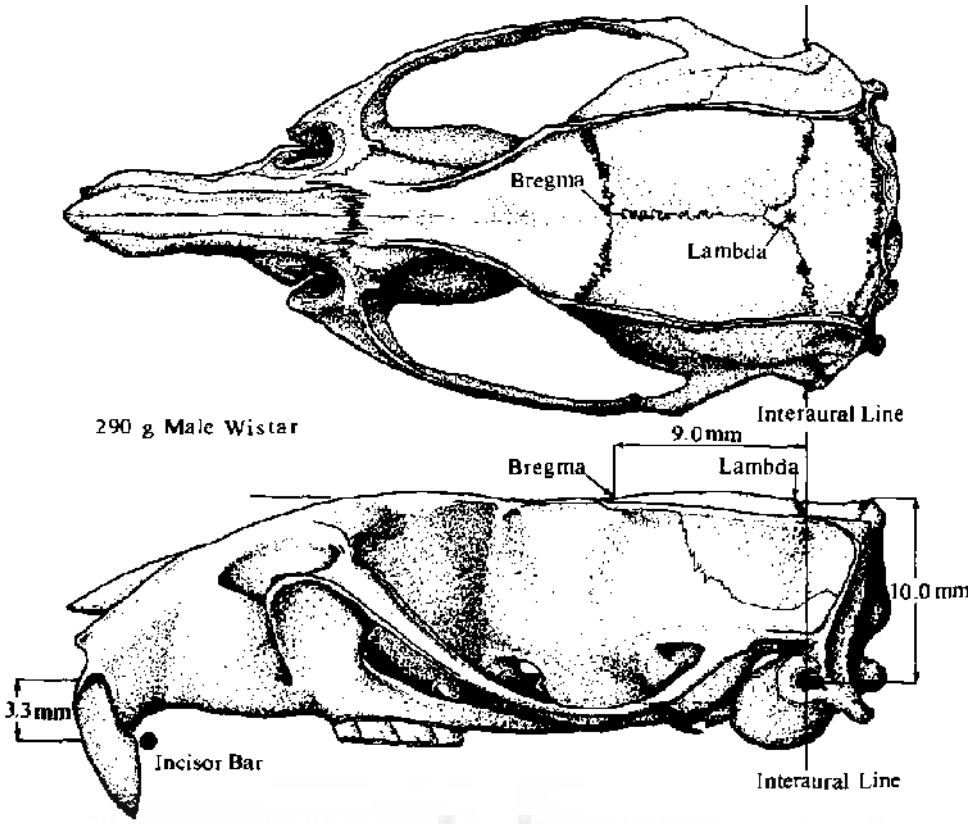

Fig. 4 Skull's stereotactic landmarks of Wistar rat (43).

The top of the head would be shaved using small animal shears, Lidocaine (Inibsa Dental, topical) would be applied to prevent the rat from experiencing pain across the area.
Then a midline incision was made parallel to the interneural line, using a scalpel exposing the periosteum and retracting the surrounding tissue.
Subsequently a small trepanation was performed using a 1.75 mm dental drill to break through the skull. Afterwards the dura mater was pierced and peeled (since it could harm the tip of the electrodes during insertion), and mineral oil was applied to the cortex to minimise brain injuries.

For the electrode implantation in V1, a stereotactic arm was placed in the stereotactic helmet, which allowed us to hold the electrode above the brain and to regulate its orientation during the subsequent insertion.

Fig. 5 Kopf Dual Small Animal Stereotaxic Instrument, Model 902 (44).

Once the electrode was perpendicularly placed in the stereotactic arm above V1, it got inserted avoiding most of the blood vessels, 1-1.5 mm deep.
Since the study was intended to compare stimulated and the non stimulated (control) brain response, the following step would only apply to the stimulated subjects.

- By using a current generator (STG1002; Multi-Channel Systems, Germany) cathodic-first biphasic current pulses were delivered to the visual cortex of 20μA or 60μA/phase (duration 180μs, 60μs of interphase interval) for 4 hours, enough time for c-Fos to express (34,45). These pulse train characteristics (e.g. 20μA and 60μA currents) were selected from previous studies where brain-electrode interaction was addressed (46).

  Afterwards, the electrode was explanted and waited an additional hour before perfusion to allow c-Fos to reach its peak of expression[12] (47).

For the non stimulated subject the process was fairly similar.

- The electrode remained implanted 4 hours (without delivering current), after which it remained for another hour. Afterwards, the electrode was slowly explanted and tested to verify its operability, followed by an additional hour before perfusion.

[12] It has been shown that this procedure is the most suitable in order to get an immune response in short periods of time for biocompatibility analysis (47).

Trans-cardially perfusion

After the fulfilment of the stimulation, the rats were sacrificed by inoculating pentobarbital (Dolethal 200 mg/kg, Vetoquinol). Afterwards, the rat was moved to a laboratory hood to perform a *trans-cardially perfusion* with phosphate-buffered saline (PBS, 7.4 pH) followed by the 4% paraformaldehyde (PFA). This process consists of exchanging blood for PBS and paraformaldehyde by placing a needle in the left ventricle of the model's heart and using the blood vessels to replace blood for PBS. Afterwards, PBS would be similarly replaced by PFA for cross-linking fixation and cell permeabilization, which would allow antibodies to access intracellular structures (48).
Afterwards, the brain was carefully extracted avoiding tissue deformation and stored submerged in 4% PFA at 4ºC.

Immunohistochemistry

Slides preparation

After surgery, it was performed the immunohistochemical staining of neurons and neuroinflammation markers such as reactive astrocytes and microglia.
The brain was cutted sagically[13] (1mm anterior to the longitudinal fissure) with a carbon steel razor blade, leaving the Ipsilateral hemisphere (where the electrode was implanted) for the creation of the tissue block. The tissue of interest was submerged in a saccharose-PBS solution (100ml of PBS and 30g saccharose per brain). The remaining tissue was stored in PFA at 4 degrees ºC for later use as a control.
The Ipsilateral stayed in the rotator at a low speed for 24 hours, which would allow the surrounding liquid to penetrate the tissue, to remove the PFA and for cryoprotection purposes. Once the brain stopped floating and plunged to the bottom (due to the higher density of the saccharose solution inside the brain), it meant that the PFA had been removed and the tissue was cryoprotected.
Next, the brain sample was taken out of the saccharose solution and placed into a cup filled with embedding medium (OCT) for 5 minutes to prepare the tissue for being cryosectioned. After that it would be placed in a mould, also with OCT for 5 minutes. After that time, the brain inside the mould was freezed by placing it inside a cage with dried ice for 5-10 minutes. This was made since fast freezing reduces cryodamage (49). Once the mould was completely frozen, it was taken to the cryostat-microtome (HM505E, Microm-Germany) to be sectioned.

The frozen block of OCT with the brain sample was taken out of the mould and pasted in a metallic stand holder which would allow to fix it and to orient it to the cryosectioning blade.

Using the cryostat microtome, the brain was sagittally sectioned with a thickness of **20 µm** and the brain slices were placed in slides.
Once the cryosectioning was completed, the tissue would be stored in a fridge at 4 degrees ºC until it would be used for immunohistochemical staining.

[13] This was made for the analysis of the electrode insertion site in V1 and the other higher visual areas.

Immunohistochemical staining

The following step would be to perform staining of c-Fos expressing neurons and neuroinflammation markers such as reactive Astrocytes and Microglia.

First, a **10% BSA[14] solution** (1g BSA/ 10ml PBT[15]) was prepared and stored in a fridge at 2-8 degrees °C to avoid microbiological activity, until the solution was homogeneous (50).

The slides were selected using a confocal microscope which would allow to identify the probe's insertion site by detecting the surrounding fluorescence. Once the tissue was selected, the slides were placed in the rotator for 10 minutes at low speed after adding **PBS** to the surface, this would allow to wash them and extract the OCT out of the tissue. This process would be repeated 3 times to completely extract the OCT.

Then prior to antibody incubation, the **BSA 10%** solution was added to the slices for 1 hour to block non-specific staining, while still being placed in the rotator at low speed.

Afterwards, the **primary antibody** was diluted in BSA 2% solution. Proportions were made according to the manufacturer's recommendation and the laboratory's previous experience.

Depending on the experimental part (**Neural activation** or **Glial activation)**, the antibodies used for tissue staining were the following:

	Cells type/Target	Primary antibody	Dilution	Secondary antibody	Dilution[16]	Colour/ Micrograph	Reference/V endor
Neural activation	Somatostatin	Somatostatin	1:200	Alexa 555 Fluor	1:100	Cyan	sc74556, SCBT
	GAD	Anti-GAD67	1:100	Alexa 555 Fluor	1:100	Magenta	Mab5406, Millipore
	Parvalbumin	Anti-Parvalbumin	1:200	Alexa 555 Fluor	1:100	Red	Ab32895, Abcam
	Neuronal nuclei	Anti-c-Fos	1:200	Alexa 488 Fluor	1:100	Green	Ab190289, Abcam
				Hoechst[17]	1:200	Blue	-
Glial activation	Astrocytes	Anti-GFAP	1:200	Alexa 555 Fluor	1:100	Red	Ab5541, Millipore
	Microglia	Anti-Iba1	1:100	Alexa 488 Fluor	1:100	Cyan	Ab178846, Abcam
	Neuronal Nuclei	Anti-NeuN	1:200	Alexa 488 Fluor	1:100	Green	ABN78, Millipore
				Hoechst	1:200	Blue	-

Table 1 Primary and secondary antibodies used for each part of the study with additional specifications.

[14] Bovine Serum Albumin (BSA, 10%, Sigma, St. Louis; MO).

[15] PBS 1-X containing 0.5% Triton-X (PBS -T).

[16] Secondary antibody's dilution was always 1:100.

[17] Hoechst was used to counterstain all slices for cell nuclei staining.

Once the hour was over (shaking the slides with BSA 10%), the **Primary antibody+BSA 2%** solution was added to chambered coverslips for a closer contact between the primary antibody and the tissue slice.

The slides now with the primary antibodies would be placed in a humid chamber[18] shaking at low speed and incubated for 24 hours at 4 degrees °C in the dark.

The day after, the chamber was removed from the slides, seeping the primary antibody. Then the tissue was washed 3 times with PBS to remove the remaining non-binded primary antibody, shaking at low speed in the dark for 10 minutes each time.
Meanwhile, the secondary antibody+BSA 2% was prepared the same way it was done for the primary antibody.
Once the slides were washed with PBS 3 times and the **secondary antibody** was diluted in BSA 2%, the antibody was placed in chambered coverslips (similar to primary antibody's methodology). Then, the slices were incubated in the dark, vibrating for **one hour** at low speed, allowing binding between secondary and primary antibodies for **1 hour.**
After that, all slides were washed 3 times with PBS taking 10 minutes per wash, removing the remaining non-binded secondary antibody.

Then, *Anti-Fade Fluorescence Mounting Medium* was added to each slice to prevent fluorescence loss. The slides were carefully covered with glass coverslips avoiding bubbles to form, especially on the tissue. The edges were sealed and all slides were stored in the dark (inside the slides box) for 7 minutes. After that, they were taken to the Apotome to perform the fluorescence imaging.

Additionally immunohistochemical staining of **glutamatergic cells** was also performed (CAMKII alpha Monoclonal Antibody (6G9), ThermoFisher Scientific. Ref: AB_325403, Dilution: 1:100. Host: Mouse). Nevertheless the results of the staining were dissatisfying.

[18] A way to maintain moisture during antibody incubation by placing wet filter paper inside the slide's cage.

Image digitisation

Apotome

After the Immunohistochemical staining, individual fluorescent tile imaging of the sagittal slices was performed by using an *ApoTome Axio Observer Z1* inverted microscope *(Carl Zeiss, Germany)* with a *10x* objective, *250-300* tiles were stitched together using the *Zen I software (Carl Zeiss)*. It is a slider module used in fluorescence microscopy that provides structured illumination allowing the generation of high-quality 2D and 3D digital images for fixed or living cells or tissues (51). It allowed the analysis of the c-Fos neurons, object-based colocalization, densitometry, glial reactivity (astrocytes and microglia) and neuronal survival.

After image processing, the resultant images were represented divided into channels as follows.

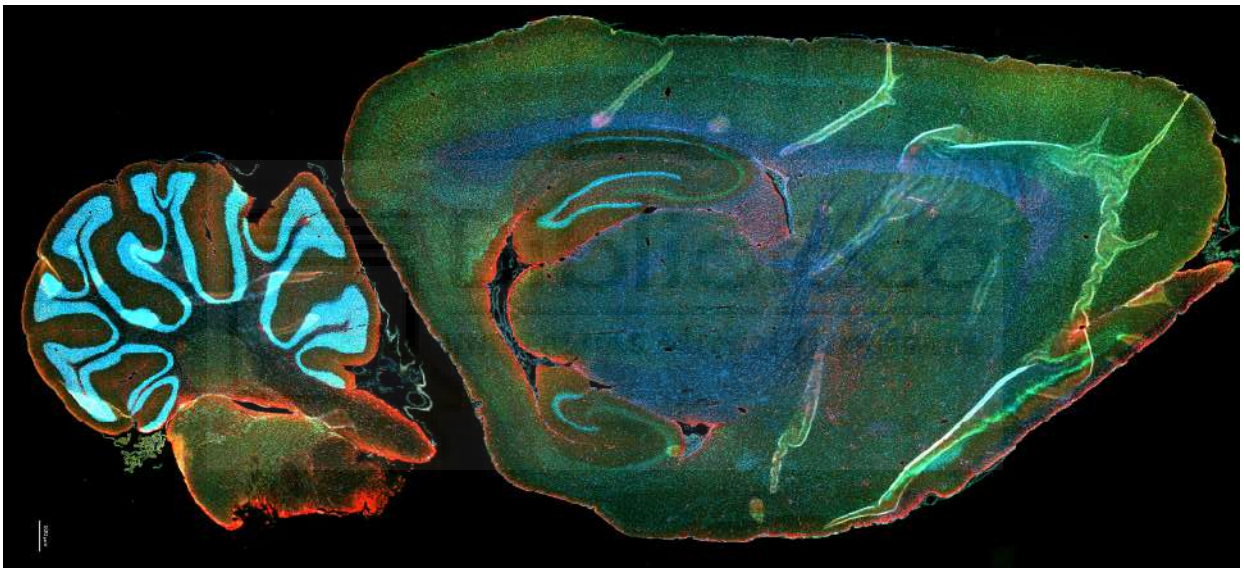

Fig. 6 Slice after performing image digitization in the ApoTome Axio Observer Z1, performed in Zen I software. The resultant image is divided into different channels according to the stained cells: GFAP (red), Iba1 (green) and Hoechst (blue).

Quantification

ImageJ-FIJI

The generated images were analysed with ImageJ-FIJI, an open source image processing package based on ImageJ[19] (52). It allowed to quantify neuron activation and glial reactivity associated with the electrode's insertion by analysing cell distribution through the different fluorescence intensity profiles around where the electrode was placed. The selected distance of quantification was the shortest from the electrode's probe to the stained cells.
For that purpose, the following steps were covered:

1. Upload the image in the database
2. Adjust the image scale by drawing a straight line on the image scale mark, and then select **Analyse>Set Scale** and there specify both the **value** and the **measure units**.
3. Dividing into the different colour channels by searching in **Image>Colour>SplitChannels**
4. Then it was selected **Image>Adjust>Threshold** to obtain the monochromatic image**.** The threshold parameters were applied in the emerging window.
5. An area quantification would be performed by drawing a square and then **Edition>Selectio>Specify>Scaled Units**. In the emerging window the size of the square would be defined, 200x200 microns. The quadrant (200x200 µm) would be placed in the cortex's surface, close to where the electrode was introduced.
6. Afterwards the quadrant angle would be adapted in order to be consistent with the probe's track in **Select>rotation**.
7. Then it would be defined the parameters of interest that are desired to get in the analysis. In this particular case, the most relevant parameter to obtain was the **Integrated Density**, however Mean and Standard deviation was also measured.
8. To get the results chart, the letter "**M**" was pressed. In order to get multiple results for different depths of the tissue, Fiji's tool "ROI Manager" was used (**Analyse>Tools>ROI Manager**). In ROI's screen the quantification quadrant was added and then, the quadrant's position would be changed to analyse different areas around where the electrode was placed, which are TOP (near the cortex), MID (in the middle of the probe), BOT (between the mid-length and the tip) and TIP. Afterwards, ROI Manager tool would generate a table with the results of the previously added parameters for all the newly added quadrants.

[19] Required plugins: FFT band pass filter, unsharp mask, threshold-triangle algorithm, ROI Manager, watershed segmentation if needed and the analyse particles command to count and measure objects

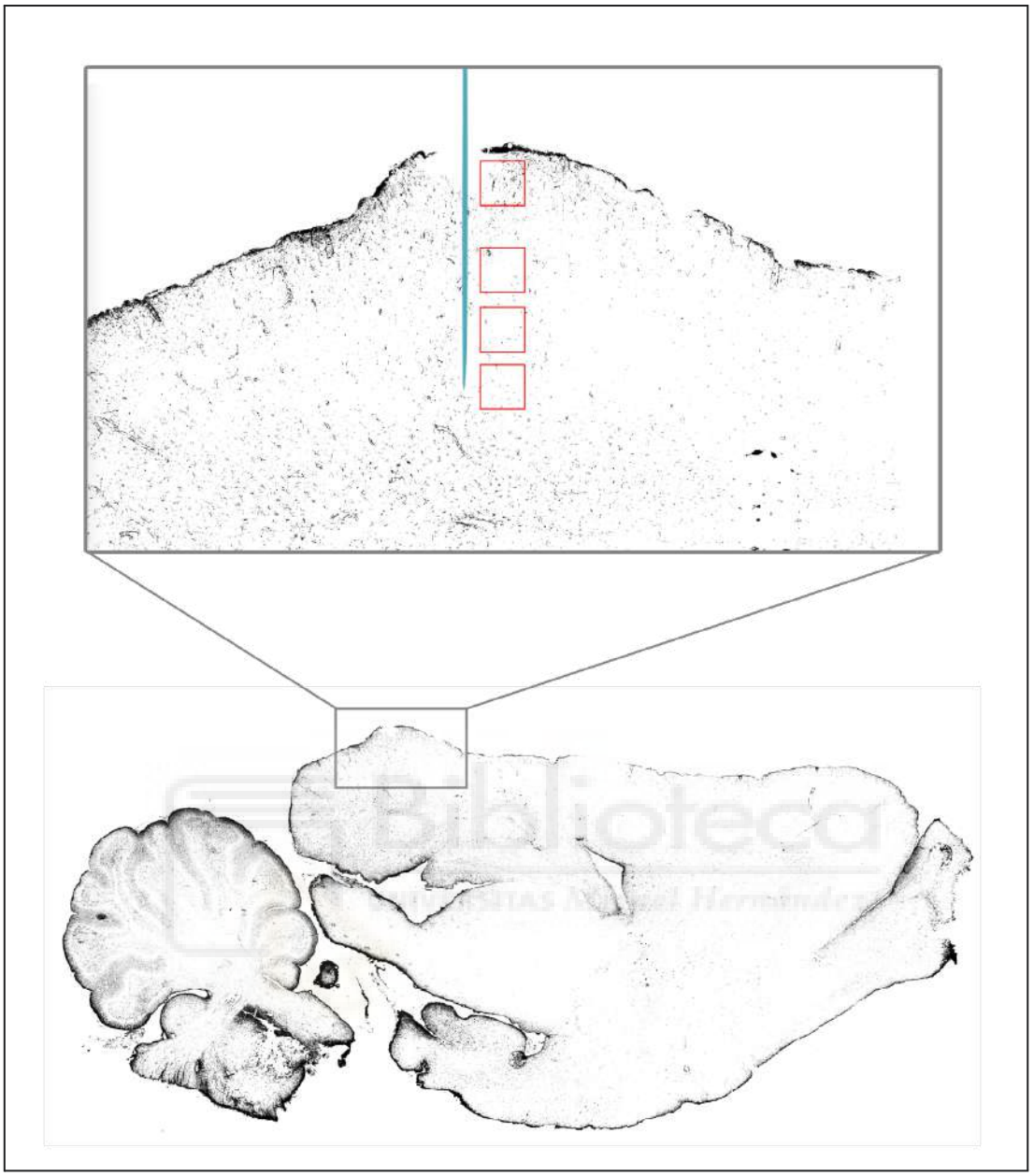

Fig. 7 Quantification with 200x200 µm quadrants (red) analysed along the inserted probe (blue) in the primary visual cortex. The brain slice shown below is the result of applying a threshold with FIJI's software.

Parameters were fed into Python, version 3.6 and data was filtered depending on each cell type.
The quantitative analysis was divided according to the following tasks:

Spatial mapping of c-Fos expressing neurons and inhibitory cellular reconstruction.
For identifying and tracking positive STT, GAD, PV and Fos neurons, some parameters were previously assessed, such as circularity (0-1), area, centroid coordinates (x,y) and mean grayscale.

Densitometry.
To perform the densitometry analysis, a Kernel Density Estimation (KDE) was performed. A KDE is a function that allows the measurement of the contribution of observations from a data sample based on the distance or their relationship using the cartesian coordinates of the filtered data for c-Fos neurons.

Object-based colocalization (OBC).

The colocalisation of c-Fos and interneurons (STT, GAD, PV) was determined by calculating the minimum Euclidean distance ($r \leq 5 \pm 2$ µm) between the centroids (x, y) of Fos neurons and interneurons.

Biocompatibility.

Mean, Standard deviation and Integrated density of relative fluorescence units (RFU) in calibrated images (µm) were quantified from the neural tissue in a 200x200µm square in the top[20], middle, bottom, and tip sections of the electrode.

Statistics

The datasets were analysed for normality distribution (Shapiro–Wilk test, $n<50$) and integrated into graphs by using GraphPad Prism 8.0.1 statistical software. The statistics were indicated as mean ± standard error and a cut-off of $p<0.05$ was applied, so in every case in which the p-value was below 0.05, the difference was considered statistically significant[21]. **Parametric** comparisons were evaluated by performing multiple comparisons via one-way ANOVA followed by a Tukey's post-hoc test or Brown-Forsythe. If data violated the assumption of homogeneity of variance, Welch's ANOVA was performed followed by Tamhane's T_2 post-hoc. **Non-parametric** comparisons were evaluated by using Mann–Whitney test.

[20] The probe's base was the top reference.

[21] Statistical significance describes how unlikely is that a difference between two variables is not due to chance.

Results

In this study, a stiff stimulating-capable electrode was implanted in V1 of rats and used to study its effect on **neural activation** and **glial activation**. To address this, three conditions were considered, **'electrode implantation with stimulation'**, **'electrode implantation without stimulation'** and **'no electrode implantation'**. For the stimulating part, two currents were considered, **20µA** and **60µA**. The types of cells studied here were **Inhibitory neurons** and **Glial cells,** and because of this, the study was addressed in two parts:

- ***Neural activation***, by using c-Fos as a neural activity marker in three cell populations: STT, GAD and PV.
- ***Glial activation*** or "Biocompatibility" analysis for the following cell types: Astrocytes and Microglia.

The following chart shows the structure that was followed across the whole experiment.

Electrode implantation with stimulation	Different currents (20µA/60µA)	Inhibitory neurons	Somatostatin (STT)
			GABA (GAD)
			Parvalbumin (PV)
		Glial cells	Astrocytes
			Microglia
Electrode implantation without stimulation	_	Inhibitory neurons	Somatostatin (STT)
			GABA (GAD)
			Parvalbumin (PV)
		Glial cells	Astrocytes
			Microglia
No electrode implantation	_	Inhibitory neurons	Somatostatin (STT)
			GABA (GAD)
			Parvalbumin (PV)

Table 2 Structure of neuron and glial activation's study.

The next step will be to address the neuron activation and glial activation.

Neuron activation

This experiment aimed to quantify the neural activity due to acute microstimulation delivered by the electrode inserted in the primary visual cortex. For that purpose neural activation was measured by using the neural activity marker c-Fos.
Since single electrode implantation unexpectedly exhibited neural activation, an additional condition was designed in order to be used as a control for further understanding of "electrode insertion without stimulation".
Cell activation was summed around the electrode insertion place across four areas near where the electrode was inserted.
The following table shows the structure followed across the current experiment.

Electrode implantation with stimulation	Different currents (20µA/60µA)	***Inhibitory neurons***	Somatostatin (STT)
			GABA (GAD)
			Parvalbumin (PV)
Control (Electrode implantation without stimulation)	_	***Inhibitory neurons***	Somatostatin (STT)
			GABA (GAD)
			Parvalbumin (PV)
Control (No electrode implantation)	_	***Inhibitory neurons***	Somatostatin (STT)
			GABA (GAD)
			Parvalbumin (PV)

Table 3 Structure of neuron activation's experiment.

In the table above (table 3) it can be seen that the experiment is divided into 3 well-defined conditions:

- *Electrode implantation **with** stimulation*
- *Electrode implantation **without** stimulation*
- *No electrode implantation*

In each one of the 3 conditions, 3 cell types were identified, ***STT, GAD and PV.***
Subsequent to performing electrode implantation and Immunohistochemistry analysis, cell populations were identified by analysing c-Fos expression. The results obtained have been gathered in the following chart.

	20µA[22]		60µA[23]		Control[24]	
	Mean	Deviation	Mean	Deviation	Mean	Deviation
STT	13	8,185	17	8,660	141,333	8,505
GAD[25]	4,333	1,527	7	5,291	117,333	32,020
PV	15,667	0,577	19	5,291	514,333	172,917
Total[26]	51,556	15,930	79	13,715	1176,333	361,929
Contralateral	4,667	2,309	3,667	2,081	9	6,658

Table 4 Mean and deviation of neuron activation for each one of the 3 conditions. The values here represent individual neurons.

Mean values shown above (table 4), were obtained out of multiple brain slices (specified in the footnote). For a stimulation of ***20µA***, a total amount of **51,556** of these neurons expressed c-Fos, and thus, exhibited activation (in an area of 160000 μm^2). From that amount, ***13*** neurons were Somatostatin, **4,333** were GABA and ***15,556*** were Parvalbumin. The remaining **18,556** activated neurons from the *Total* correspond to other neuron types, however since they are not part of this study's purpose, their characteristics remain unknown.

On the other hand, in the contralateral side (opposite brain hemisphere to the electrode insertion) of the brain only **4,667** neurons showed activation, significantly less than in the Ipsilateral side (brain hemisphere where the electrode was implanted).

Last column named *"no stimulation"* shows that insertion of the electrode triggered a substantial increase for all the neuron populations.

All three neuron populations exhibited increased activity the higher the stimulation was. But all of them also exhibited higher activity with electrode insertion compared to electrical stimulation.

This phenomenon's interpretation is that electrical stimulation activates all kinds of neurons, including inhibitory neurons (STT, GAD and PV), and when these get stimulated they inhibit other neurons nearby, thus substantially decreasing the number of activated neurons.

[22] Values were obtained out of all Ipsilateral slices / 9 Contralateral slices.

[23] Values were obtained out of all Ipsilateral slices / 9 Contralateral slices.

[24] Values were obtained out of all Ipsilateral slices / 9 Contralateral slices.

[25] GABA is primarily synthesised from glutamate and catalysed by glutamate decarboxylase (GAD) (https://www.abcam.com/neuroscience/gabaergic-neuron-markers-and-their-functions).

[26] The *Total* row excludes the *Contralateral* results.

	20µA	60µA	Control
STT	25,21%	21,51%	12,01%
GAD	8,4%	8,86%	9,97%
PV	30,388%	24%	43,72%
Unknown	36%	45,63%	34,3%

Table 5 Neuron activation representativeness around the electrode with respect to the *Total*.

In the chart above (table 5), the percentages shown correspond to each activated neuron type out of the *Total* c-Fos expressing nucleus (table 4). It was calculated by comparing each cell population with the *Total value*.

It can be seen that **GAD** always exhibited **lower activity** compared to STT and PV neurons.

It should also be noted that **Parvalbumin** cells exhibited significantly **higher activity** predominance when **no stimulation** was being delivered.

Here the *Unknown* category represents the percentage of c-Fos expressing cells different from Somatostatin, GAD or Parvalbumin in the tissue.

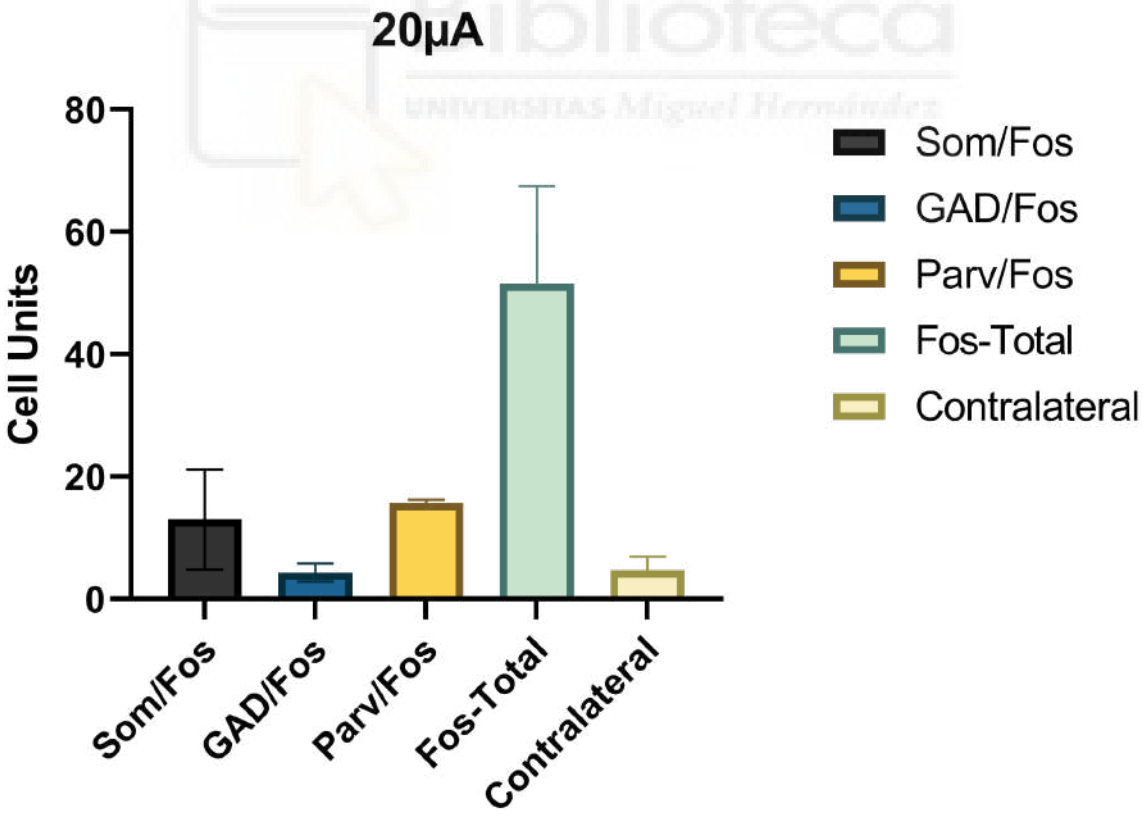

Fig. 8 Neuron activation associated with a **20µA** stimulation.

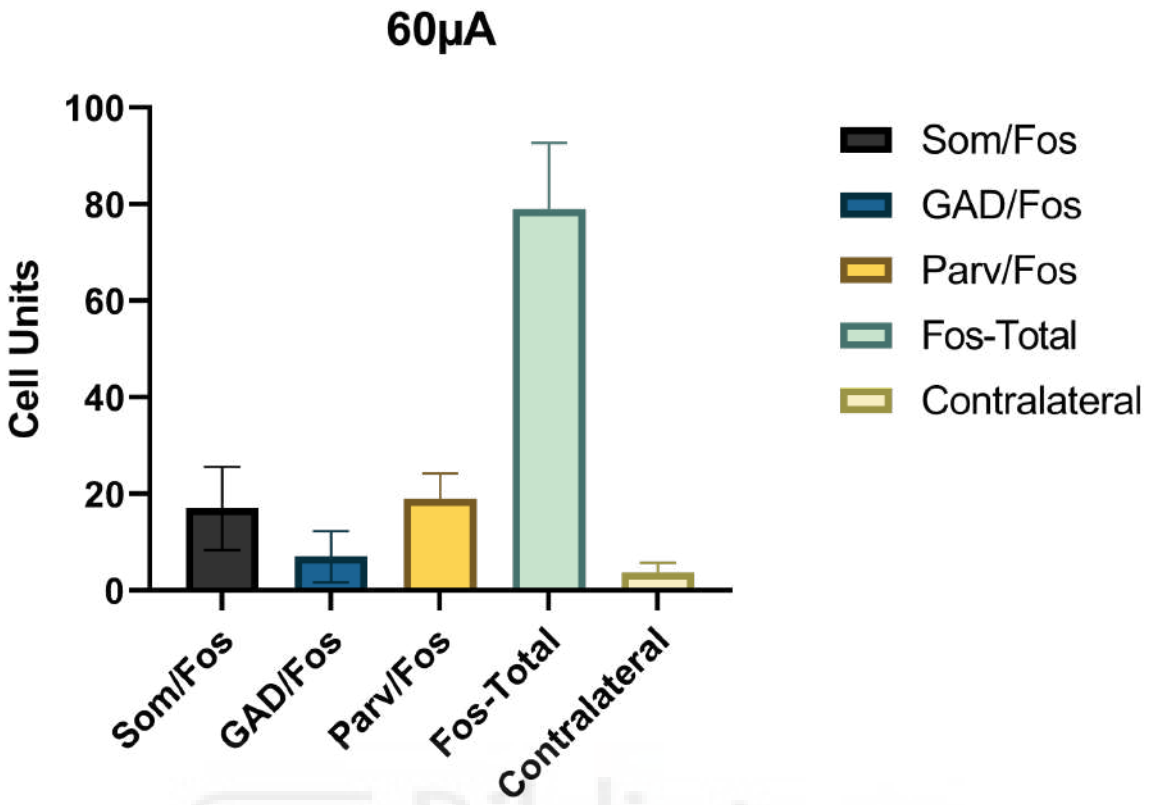

Fig. 9 Neuron activation associated with a 60µA stimulation.

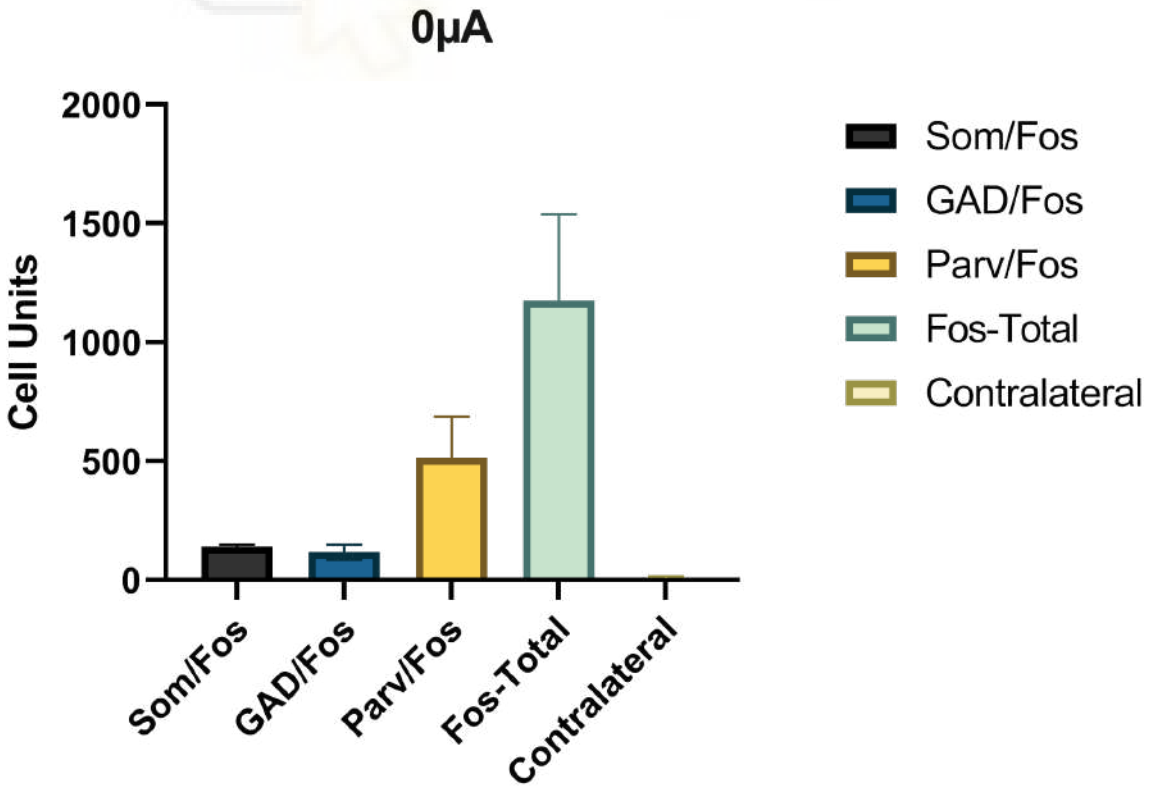

Fig. 10 Control (Neuron activation **without** stimulation).

The graphs above (fig.8-10) show neuron activation results (table 4) for each one of the three conditions. The results show that by inserting the electrode **without stimulation,** inhibitory neurons exhibited **significantly higher activity than stimulating** (fig. 8, fig.9), even at the contralateral there was a slight activation increase but not as significant.

Glial activation (Biocompatibility)

The biocompatibility analysis was addressed by quantifying glial cell activation (Astrocytes and Microglia) following the same three conditions mentioned above (table 3) without the control without electrode implantation.
The following table's aims to provide a clear view of the experiment's structure.

Electrode implantation with stimulation	Different currents (20µA/60µA)	***Glial cells***	Astrocytes
			Microglia
Electrode implantation without stimulation (Control)	_	***Glial cells***	Astrocytes
			Microglia

Table 6 Structure of glial activation's experiment.

It can be seen that the experiment is divided into the same 3 specific conditions, and for each one of them 2 glial cell types were identified, Astrocytes and Microglia.
Subsequent to performing Immunohistochemistry analysis, these cells were identified. The results obtained have been gathered in the following chart.

	20µA[27]		60µA[28]		Control[29]	
	Mean	Deviation	Mean	Deviation	Mean	Deviation
Astrocytes	975,418	25,153	985,011	15,755	987,013	8,110
Microglia	957,706	9,674	970,814	10,925	1011,528	4,470
Total[30]	1933,124	34,827	1955,825	26,680	1998,541	12,580

Table 7 Mean and deviation of glial activation for each one of the 3 conditions. The mean values represent fluorescence detected in the four quantification quadrants (200x200 µm).

The values shown in the table above (table 7) correspond to the Mean and Standard Deviation obtained after quantifying multiple brain slices[31]. The results show a clear **increase** in glial activation, for both cell populations (Astrocytes and Microglia) around the electrode for every situation.
For a stimulation of ***20µA***, the amount of Astrocytes around the electrode represented a Mean value of 975,418. For the same stimulation, Microglia population around the electrode represented a Mean value of 957,706.
For a stimulation of ***60µA***, the amount of Astrocytes around the electrode represented a Mean value of 985,011. For the same stimulation, Microglia population around the electrode represented a value of 970,814.
Lastly, with the electrode inserted without stimulation, the amount of Astrocytes around the electrode represented a Mean value of 987,013. Microglia represented a mean of 1011,528**.** Both glial populations exhibited a slight increase in the presence of both cell populations around the electrode when **no stimulation** was being delivered.

	20µA	60µA	Control
Astrocytes	50,458%	50,363%	49,386%
Microglia	49,542%	49,637%	50,613%

Table 8 Glial activation representativeness around the electrode with respect to the *Total*.

The table above (table 8) represents the percentage of each glial population's presence around the electrode. **Astrocytes** exhibited slightly **higher activity around** the electrode every time **stimulation** was being **delivered,** compared to Microglia. On the other hand, **Microglia's** activity around the electrode

[27] Mean and Deviation values were obtained from 7 slices for Astrocytes and 4 for Microglia.
[28] Mean and Deviation values were obtained from 6 slices for Astrocytes and 4 for Microglia.
[29] Mean and Deviation values were obtained from 6 slices for Astrocytes and 4 for Microglia.
[30] Astrocytes + Microglia
[31] For 60µA and the 0µA groups, Mean and Deviation values were obtained from 6 slices for Astrocytes and 4 for Microglia. For 20µA Mean and Deviation values were obtained from 7 slices for Astrocytes and 4 for Microglia.

was slightly higher when **stimulation was not being delivered**, representing 50,613% of the total glial response (without stimulation) compared to the Astrocytes, representing 49,386%.

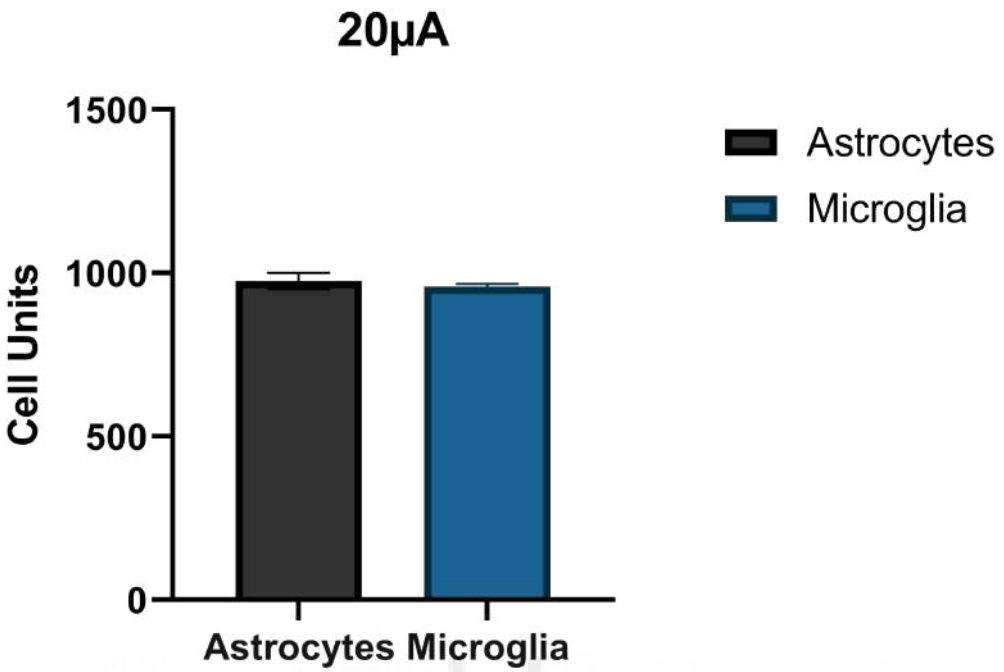

Fig. 11 Glial activation with a **20µA** stimulation.

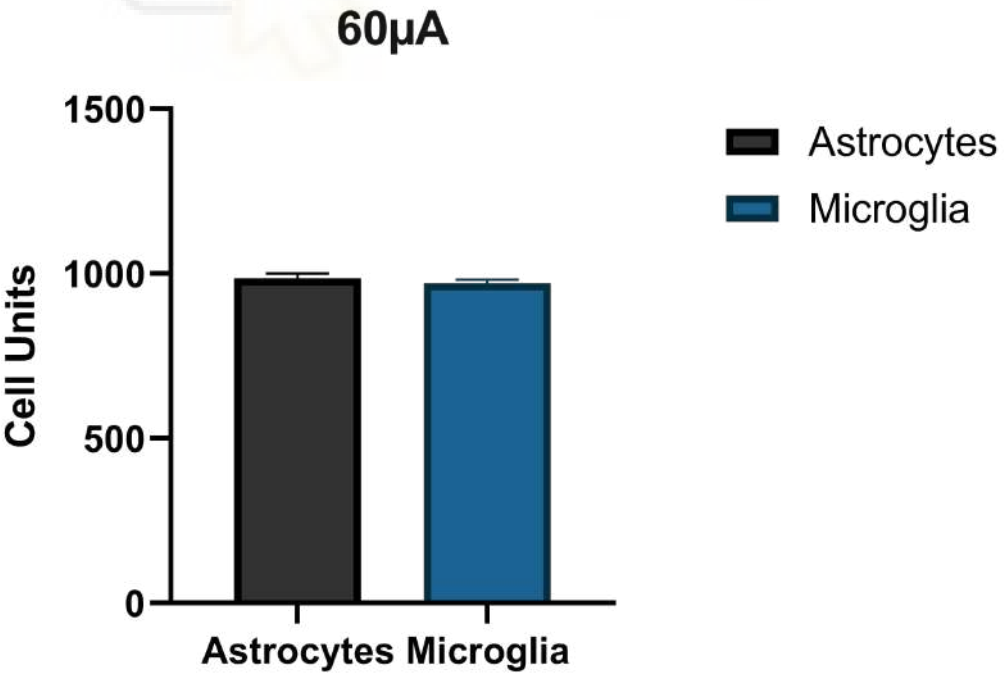

Fig. 12 Glial activation with a **60µA** stimulation.

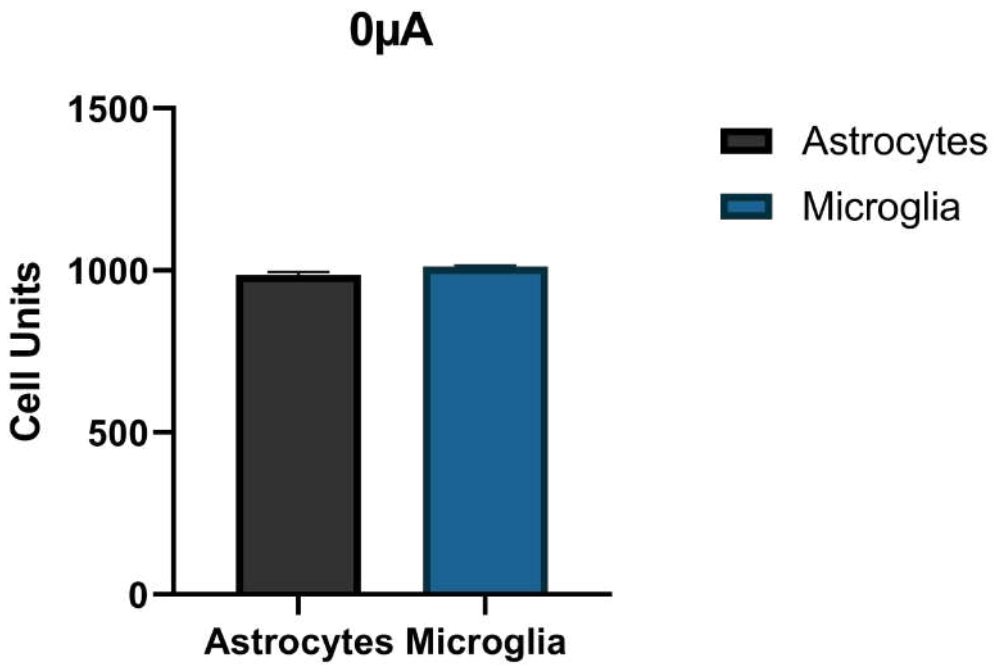

Fig. 13 Glial activation **without** stimulation (Control).

The graphs above (fig. 11-13) show the glial response for each one of the three situations. The results show that by inserting the electrode **without stimulation,** glial populations exhibited **slightly higher activity** compared to when stimulation was being delivered.

	Brown-Forsythe and Welch ANOVA tests					
1	Table Analyzed	GFAP				
2						
3	**Brown-Forsythe ANOVA test**					
4	F* (DFn, DFd)	0.7682 (2.000, 11.08)				
5	P value	0.4870				
6	P value summary	ns				
7	Significant diff. among means (P < 0.05)?	No				
8						
9	**Welch's ANOVA test**					
10	W (DFn, DFd)	0.5714 (2.000, 8.589)				
11	P value	0.5848				
12	P value summary	ns				
13	Significant diff. among means (P < 0.05)?	No				
14						
15	**Data summary**					
16	Number of treatments (columns)	3				
17	Number of values (total)	24				

Table. 12 Brown-Forsythe and Welch ANOVA tests for Astrocytes (not statistically significant).

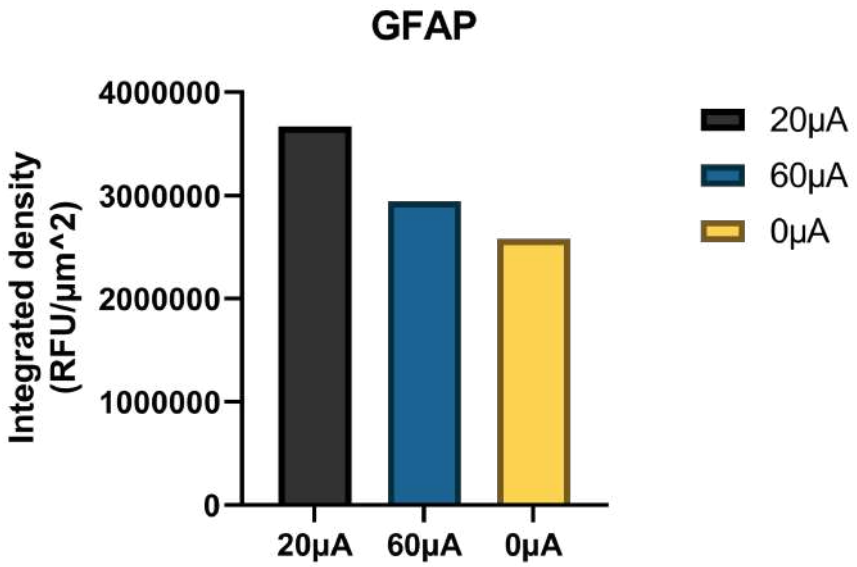

Fig. 14 Glial activation **without** stimulation (Control). The area where the values were obtained was across the 4 quantification quadrants (200x200 µm).

It was however not possible to draw a **statistically significant conclusion** on Astrocytes activation associated to microstimulating with an intracortical electrode in V1, since *P-value* (0.4870) was higher than 0,05 (0.477>0.05).

	Brown-Forsythe and Welch ANOVA tests					
1	Table Analyzed	Iba1				
2						
3	**Brown-Forsythe ANOVA test**					
4	F* (DFn, DFd)	34.06 (2.000, 6.813)				
5	P value	0.0003				
6	P value summary	***				
7	Significant diff. among means (P < 0.05)?	Yes				
8						
9	**Welch's ANOVA test**					
10	W (DFn, DFd)	46.33 (2.000, 4.945)				
11	P value	0.0006				
12	P value summary	***				
13	Significant diff. among means (P < 0.05)?	Yes				
14						
15	**Data summary**					
16	Number of treatments (columns)	3				
17	Number of values (total)	13				

Table. 13 Brown-Forsythe and Welch ANOVA tests for Microglia (statistically significant).

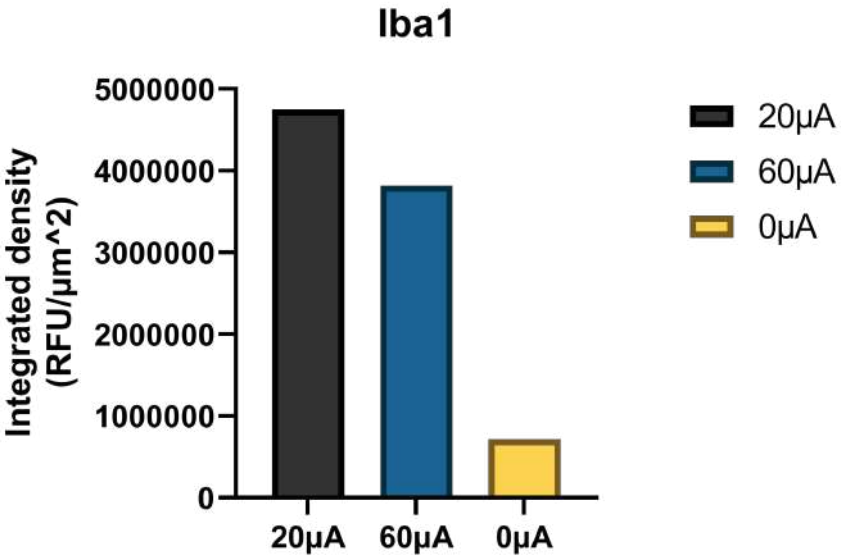

Fig. 15 Glial activation **without** stimulation (Control). The area where the values were obtained was across the four quantification quadrants (200x200 µm).

In contrast with Astrocytes, in the case of Microglia it was possible to draw a **statistically significant conclusion** on its activation associated to microstimulation with an intracortical electrode in V1, since *P-value* (0,0003) was lower than 0,05 (0,0003<0,05).

Discussion and conclusions

Neuron activation

The study covered 4 hours of acute microstimulation which is considered to be representative since it is enough time for c-Fos to express. Data collected over this time frame indicated that there is a correlation between **acute microstimulation level** in the primary visual cortex of rats, and an increased **neuron activation** in the electrode sites. However, the control group (electrode insertion) exhibited substantially more activation.

Moreover, it has been discovered that the insertion of stimulating-capable electrodes in the cortex exhibit neuron activation without current delivery. The differences between the two applied currents (20µA and 60µA) and the **non-stimulating** part were presumably influenced by, the neuron-inhibition effect due to inhibitory neuron stimulation, and the neuron-excitatory effect due to excitatory neuron stimulation. Still, this cannot be concluded, mainly for the lack of data regarding the activated excitatory neurons.

Neuron activation associated with **electrode insertion without stimulation** was unexpectedly high (1176,333 neurons).

It should also be noticed that during stimulation **all neurons** exhibited a **direct stimulating-activation relationship.** Lower electrical stimulation (20µA) exhibited lower neuron activation, compared to the higher electrical stimulation (60µA). More efforts should be made to elucidate how acute microstimulation influences neural activation by delivering higher currents (>60µA) and lower currents (<20µA) to determine if that direct stimulating-activation relationship is maintained.

Nonetheless, these results were considered **not statistically significant**[32]**.**

Furthermore, it appears to be that c-Fos expression could be influenced by other variables, such as Anaesthesia. It has previously been suggested from in vivo studies (53) that c-Fos expression could be associated with high Isoflurane concentration during surgery. This event did not influence our results since our Anaesthesia concentrations were the same for all the experimental conditions. It would be positive to further research this event to elucidate how c-Fos expression is associated with different Anaesthesia exposure or brain damage, as well as addressing c-Fos expression associated to electrical stimulation for longer periods than 4 hours, being able to study the effects of an abiding use more accurately (34,47).

Glial activation

Regarding glial reactivity, immune response associated with acute **microstimulation** exhibited higher glial activation around the implanted area. However, higher current stimulation exhibited lower glial activation.

As to **electrode insertion without stimulation**, slightly lower glial activation was detected compared to when current was being delivered.

During stimulation, all glial cells exhibited a **direct stimulation-activation relationship** exhibiting more activation as the current increased. Higher electrical stimulation (60µA) exhibited higher glial activation, compared to the lower electrical stimulation (20µA). More efforts should be made to elucidate how acute microstimulation influences glial activation by delivering higher currents (>60µA) and lower currents (<20µA) to determine if that direct stimulating-activation relationship is maintained.

[32] By using a cut-off of $P<0.05$

Nonetheless, these results were considered **not statistically significant** regarding Astrocytes activation but **statistically significant** regarding Microglia activation.
It would be positive to further research glial reactivity associated with **electrode's insertion** and to **acute microstimulation** for longer than 4 hours in order to understand more profoundly how glial cells would interact with the electrode in the long term. This could help to elucidate how to minimise brain immune response, to estimate more accurately the long term performance and biocompatibility.

Bibliography

1. Chen X, Wang F, Fernandez E, Roelfsema PR. Shape perception via a high-channel-count neuroprosthesis in monkey visual cortex. Science [Internet]. 2020 Dec 4;370(6521):1191–6. Available from: http://dx.doi.org/10.1126/science.abd7435

2. About Blindness and partial Sight - Facts and figures [Internet]. [cited 2022 May 1]. Available from: https://www.euroblind.org/about-blindness-and-partial-sight/facts-and-figures

3. Brennan I. Visual pathway and visual field defects [Internet]. Geeky Medics. 2020 [cited 2022 May 1]. Available from: https://geekymedics.com/visual-pathway-and-visual-field-defects/

4. Lozano A, Suárez JS, Soto-Sánchez C, Garrigós J, Martínez-Alvarez JJ, Ferrández JM, et al. Neurolight: A Deep Learning Neural Interface for Cortical Visual Prostheses. Int J Neural Syst [Internet]. 2020 Sep 1;30(09):2050045. Available from: https://doi.org/10.1142/S0129065720500458

5. Wikipedia contributors. Phosphene [Internet]. Wikipedia, The Free Encyclopedia. 2022. Available from: https://en.wikipedia.org/w/index.php?title=Phosphene&oldid=1075717579

6. Fernandez E, Normann R. Introduction to Visual Prostheses. In: Kolb H, Fernandez E, Nelson R, editors. Webvision: The Organization of the Retina and Visual System [Internet]. Salt Lake City (UT): University of Utah Health Sciences Center; 2016. Available from: https://www.ncbi.nlm.nih.gov/pubmed/27809426

7. Visual prosthesis Implant Microcoil Technology, Lee Seung Gi, angle, text, material png [Internet]. [cited 2022 May 2]. Available from: https://www.pngwing.com/en/free-png-xneck

8. Saldanha RL, Urdaneta ME, Otto KJ. The Role of Electrode-Site Placement in the Long-Term Stability of Intracortical Microstimulation. Front Neurosci [Internet]. 2021 Sep 8;15:712578. Available from: http://dx.doi.org/10.3389/fnins.2021.712578

9. Buzsáki G. Large-scale recording of neuronal ensembles. Nat Neurosci [Internet]. 2004 Apr 27 [cited 2022 Aug 21];7(5):446–51. Available from: https://www.nature.com/articles/nn1233

10. Neuroscience [Internet]. BrainGate. 2015 [cited 2022 May 8]. Available from: https://www.braingate.org/research-areas/neuroscience/

11. Rapinesi C, Kotzalidis GD, Ferracuti S, Sani G, Girardi P, Del Casale A. Brain Stimulation in Obsessive-Compulsive Disorder (OCD): A Systematic Review. Curr Neuropharmacol [Internet]. 2019;17(8):787–807. Available from: http://dx.doi.org/10.2174/1570159X17666190409142555

12. Salanova V. Deep brain stimulation for epilepsy. Epilepsy Behav [Internet]. 2018 Nov;88S:21–4. Available from: http://dx.doi.org/10.1016/j.yebeh.2018.06.041

13. Limousin P, Foltynie T. Long-term outcomes of deep brain stimulation in Parkinson disease. Nat Rev Neurol [Internet]. 2019 Apr;15(4):234–42. Available from: http://dx.doi.org/10.1038/s41582-019-0145-9

14. Products - Blackrock Neurotech (Research) [Internet]. Blackrock Neurotech (Research). 2020 [cited 2022 May 21]. Available from: https://blackrockneurotech.com/research/products/?gclid=Cj0KCQjwr4eYBhDrARIsANPywChKOa6Y14UXOlHSDWUyv76nJRdu2Ki95GLdbs8rkXauVatm9nzewcIaAngoEALw_wcB

15. HajjHassan M, Chodavarapu V, Musallam S. NeuroMEMS: Neural Probe Microtechnologies. Sensors [Internet]. 2008 Oct 25;8(10):6704–26. Available from: http://dx.doi.org/10.3390/s8106704

16. Seo KJ, Artoni P, Qiang Y, Zhong Y, Han X, Shi Z, et al. Transparent, Flexible, Penetrating Microelectrode Arrays with Capabilities of Single-Unit Electrophysiology. Adv Biosyst [Internet]. 2019 Mar;3(3):e1800276. Available from: http://dx.doi.org/10.1002/adbi.201800276

17. Normann RA, Fernandez E. Clinical applications of penetrating neural interfaces and Utah Electrode Array technologies. J Neural Eng [Internet]. 2016 Dec;13(6):061003. Available from: http://dx.doi.org/10.1088/1741-2560/13/6/061003

18. Shi D, Dhawan V, Cui XT. Bio-integrative design of the neural tissue-device interface. Curr Opin Biotechnol [Internet]. 2021 Dec;72:54–61. Available from: http://dx.doi.org/10.1016/j.copbio.2021.10.003

19. Shi Z. Penetrating Arrays of Transparent, Flexible Bilayer-nanomesh Microelectrodes with Capabilities of Single Unit Electrophysiology [Internet]. 2020. Available from:

https://search.proquest.com/openview/236585f4928afb124670a49ed62e0eec/1?pq-origsite=gscholar&cbl=44156

20. Bedell HW, Song S, Li X, Molinich E, Lin S, Stiller A, et al. Understanding the Effects of Both CD14-Mediated Innate Immunity and Device/Tissue Mechanical Mismatch in the Neuroinflammatory Response to Intracortical Microelectrodes. Front Neurosci [Internet]. 2018 Oct 31;12:772. Available from: http://dx.doi.org/10.3389/fnins.2018.00772

21. Álvarez E, González B, Lozano D, Doadrio AL, Colilla M, Izquierdo-Barba I. Nanoantibiotics Based in Mesoporous Silica Nanoparticles: New Formulations for Bacterial Infection Treatment. Pharmaceutics [Internet]. 2021 Nov 29;13(12). Available from: http://dx.doi.org/10.3390/pharmaceutics13122033

22. Boehler C, Kleber C, Martini N, Xie Y, Dryg I, Stieglitz T, et al. Actively controlled release of Dexamethasone from neural microelectrodes in a chronic in vivo study. Biomaterials [Internet]. 2017 Jun;129:176–87. Available from: http://dx.doi.org/10.1016/j.biomaterials.2017.03.019

23. Fernández E, Botella P. Biotolerability of intracortical microelectrodes. Adv Biosyst [Internet]. 2018 Jan;2(1):1700115. Available from: https://onlinelibrary.wiley.com/doi/10.1002/adbi.201700115

24. Xu JC, Fan J, Wang X, Eacker SM, Kam TI, Chen L, et al. Cultured networks of excitatory projection neurons and inhibitory interneurons for studying human cortical neurotoxicity. Sci Transl Med [Internet]. 2016 Apr 6;8(333):333ra48. Available from: http://dx.doi.org/10.1126/scitranslmed.aad0623

25. Lakna. Difference between excitatory and inhibitory neurons [Internet]. Pediaa.Com. 2018 [cited 2022 May 8]. Available from: https://pediaa.com/difference-between-excitatory-and-inhibitory-neurons/

26. Sultan KT, Shi SH. Generation of diverse cortical inhibitory interneurons. Wiley Interdiscip Rev Dev Biol [Internet]. 2018 Mar;7(2). Available from: http://dx.doi.org/10.1002/wdev.306

27. Bélanger M, Magistretti PJ. The role of astroglia in neuroprotection. Dialogues Clin Neurosci [Internet]. 2009;11(3):281–95. Available from: https://www.ncbi.nlm.nih.gov/pubmed/19877496

28. Wake H, Moorhouse AJ, Nabekura J. Functions of microglia in the central nervous system--beyond the immune response. Neuron Glia Biol [Internet]. 2011 Feb;7(1):47–53. Available from: http://dx.doi.org/10.1017/S1740925X12000063

29. Ludwig PE, Reddy V, Varacallo M. Neuroanatomy, Neurons. In: StatPearls [Internet]. Treasure Island (FL): StatPearls Publishing; 2021. Available from: https://www.ncbi.nlm.nih.gov/pubmed/28723006

30. De Silva TM, Faraci FM. Hypertension. In: Primer on Cerebrovascular Diseases [Internet]. Elsevier; 2017. p. 153–7. Available from: https://www.sciencedirect.com/topics/neuroscience/neurovascular-coupling

31. Heumann R, Goemans C, Bartsch D, Lingenhöhl K, Waldmeier PC, Hengerer B, et al. Transgenic activation of Ras in neurons promotes hypertrophy and protects from lesion-induced degeneration. J Cell Biol [Internet]. 2000 Dec 25;151(7):1537–48. Available from: http://dx.doi.org/10.1083/jcb.151.7.1537

32. Ohsawa K, Kohsaka S. Microglial Response to Injury. In: Encyclopedia of Neuroscience [Internet]. Elsevier; 2009. p. 861–4. Available from: https://www.sciencedirect.com/topics/neuroscience/neuronal-cell-death

33. Bullitt E. Expression of c-fos-like protein as a marker for neuronal activity following noxious stimulation in the rat. J Comp Neurol [Internet]. 1990 Jun 22;296(4):517–30. Available from: http://dx.doi.org/10.1002/cne.902960402

34. Herrera, Robertson. Activation of c-fos in the brain. Prog Neurobiol [Internet]. Available from: https://www.sciencedirect.com/science/article/pii/S0301008296000214?casa_token=AIKKe6kSWgYAAAAA:3BxPEhPMtw9emhgucrOHCkbXG_40c2t_geAvPvJqOfARJz-LSu5xnmArqXj0vVTlMeyDcCqm

35. Wikipedia contributors. Visual cortex [Internet]. Wikipedia, The Free Encyclopedia. 2022. Available from: https://en.wikipedia.org/w/index.php?title=Visual_cortex&oldid=1097288750

36. Potter KA, Simon JS, Velagapudi B, Capadona JR. Reduction of autofluorescence at the microelectrode-cortical tissue interface improves antibody detection. J Neurosci Methods [Internet]. 2012 Jan 15;203(1):96–105. Available from: http://dx.doi.org/10.1016/j.jneumeth.2011.09.024

37. Harris JP, Hess AE, Rowan SJ, Weder C, Zorman CA, Tyler DJ, et al. In vivo deployment of mechanically adaptive nanocomposites for intracortical microelectrodes. J Neural Eng [Internet]. 2011 Aug;8(4):046010. Available from: http://dx.doi.org/10.1088/1741-2560/8/4/046010

38. Soto-Sánchez C, Martínez-Navarrete G, Humphreys L, Puras G, Zarate J, Pedraz JL, et al. Enduring high-efficiency in vivo transfection of neurons with non-viral magnetoparticles in the rat visual cortex for

optogenetic applications. Nanomedicine [Internet]. 2015 May;11(4):835–43. Available from: http://dx.doi.org/10.1016/j.nano.2015.01.012

39. Platinum-iridium bipolar electrodes, blunted tip [Internet]. [cited 2022 Sep 4]. Available from: https://science-products.com/en/shop/395/78/electrodes-etc/metal-microelectrodes/bipolar/bipolar-pt-bt

40. Why warmth matters before, during and after surgery [Internet]. [cited 2022 May 27]. Available from: https://www.3m.com/3M/en_US/particles/all-articles/article-detail/~/hypothermia-body-temperature-perioperative-comfort-feeling-cold-after-surgery/?storyid=464a5be8-b0e3-4b57-b2ff-3151dd4af66b

41. Sapru HN, Krieger AJ. Carotid and aortic chemoreceptor function in the rat. J Appl Physiol [Internet]. 1977 Mar;42(3):344–8. Available from: https://sci-hub.hkvisa.net/10.1152/jappl.1977.42.3.344

42. Wikipedia contributors. Bregma [Internet]. Wikipedia, The Free Encyclopedia. 2021. Available from: https://en.wikipedia.org/w/index.php?title=Bregma&oldid=1037742743

43. Espinosa-Oliva AM, de Pablos R, Herrera AJ, Zakaria R, Yaacob WMH, Othman Z, et al. Fig. 1 (a) Diagram showing the three stereotaxic coordinates and the [Internet]. ResearchGate. 2013 [cited 2022 Aug 29]. Available from: https://www.researchgate.net/figure/a-Diagram-showing-the-three-stereotaxic-coordinates-and-the-structures-at-56-mm_fig1_243968948

44. Model 900LS small animal stereotaxic instrument [Internet]. [cited 2022 Sep 1]. Available from: https://kopfinstruments.com/product/model-900ls-small-animal-stereotaxic-instrument/

45. Sagar SM, Sharp FR, Curran T. Expression of c-fos protein in brain: metabolic mapping at the cellular level. Science [Internet]. 1988 Jun 3;240(4857):1328–31. Available from: http://dx.doi.org/10.1126/science.3131879

46. Fernández E, Alfaro A, Soto-Sánchez C, Gonzalez-Lopez P, Lozano AM, Peña S, et al. Visual percepts evoked with an intracortical 96-channel microelectrode array inserted in human occipital cortex. J Clin Invest [Internet]. 2021 Dec 1;131(23). Available from: http://dx.doi.org/10.1172/JCI151331

47. Schulte T, Brecht S, Herdegen T, Illert M, Mehdorn HM, Hamel W. Induction of immediate early gene expression by high-frequency stimulation of the subthalamic nucleus in rats. Neuroscience [Internet]. 2006 Feb 7;138(4):1377–85. Available from: http://dx.doi.org/10.1016/j.neuroscience.2005.12.034

48. Chang KM, Ho L, Freshney RI, Gray P. Principle behind cell fixation? [Internet]. ResearchGate. 2003 [cited 2022 May 27]. Available from: https://www.researchgate.net/post/Principle-behind-cell-fixation

49. Roberts K, Tuck L. Embedding and freezing fresh human tissue in OCT using isopentane v2 [Internet]. 2019 [cited 2022 May 28]. Available from: https://www.protocols.io/view/embedding-and-freezing-fresh-human-tissue-in-oct-u-bp2l64o55vqe/v3

50. Mitchell R. 7 tips for suspending BSA in solution [Internet]. Lab Manager. Lab Manager Magazine; 2017 [cited 2022 May 28]. Available from: https://www.labmanager.com/insights/7-tips-for-suspending-bsa-in-solution-7199

51. Bioelektronik (IBI-3) [Internet]. [cited 2022 May 29]. Available from: https://www.fz-juelich.de/ibi/ibi-3/EN/Expertise/02-InstrumentationMethods/ApoTome/_node.html

52. Wikipedia contributors. Fiji (software) [Internet]. Wikipedia, The Free Encyclopedia. 2022. Available from: https://en.wikipedia.org/w/index.php?title=Fiji_(software)&oldid=1077271570

53. Zhang D, Liu J, Zhu T, Zhou C. Identifying c-fos Expression as a Strategy to Investigate the Actions of General Anesthetics on the Central Nervous System. Curr Neuropharmacol [Internet]. 2022;20(1):55–71. Available from: http://dx.doi.org/10.2174/1570159X19666210909150200